Electrochemical Reduction of Bisulfite in Mildly Acidic Buffers: Kinetics of Sulfur Dioxide−Bisulfite Interconversion

Yuriy V. Tolmachev and Daniel A. Scherson*

Department of Chemistry and Ernest B. Yeager Center for Electrochemical Sciences, Case Western Reserve University, Cleveland, Ohio 44106-7078

Received: September 17, 1998; In Final Form: December 30, 1998

The reduction of bisulfite on a bismuth rotating disk electrode (RDE) was studied in aqueous buffered electrolytes over the pH range 3−6. Clearly defined limiting currents were observed in all solutions examined; however, their magnitudes were not only smaller than those expected for a process limited by the diffusion of bisulfite from the bulk solution, but were also found to decrease as the media became less acidic. This behavior was attributed to a preceding homogeneous process that generates sulfur dioxide, the actual electroactive species. UV−visible absorption−reflection spectroscopy measurements at a RDE showed that in the potential region in which such limiting currents are observed, dithionite is produced with 100% faradaic efficiency. Results of rotation rate staircase scan amperometric RDE experiments were found to be consistent with the conversion of bisulfite into SO_2 proceeding via a general acid catalysis mechanism, and allowed values for the rate constants for the following reactions to be determined: $SO_2 + H_2O \rightarrow HSO_3^- + H_3O^+$, $k_b = (1.6 \pm 0.2)\ 10^7\ s^{-1}$; $HSO_3^- + H_3O^+ \rightarrow SO_2 + H_2O$, $k_f^H = (1.2 \pm 0.15)\ 10^9\ M^{-1}\ s^{-1}$; $HSO_3^- + CH_3COOH \rightarrow SO_2 + H_2O + CH_3COO^-$, $k_f^{HA} = (1.7 \pm 0.5)\ 10^4\ M^{-1}\ s^{-1}$. On this basis, and assuming diffusion-controlled rates for proton transfer from strong acids to oxygen bases, a more detailed mechanism involving formation of sulfurous acid as an intermediate is discussed and some thermodynamic and kinetic properties of the latter are estimated.

Introduction

The electrochemical reduction of bisulfite in aqueous electrolytes has received renewed attention in recent years prompted by the advantages this process offers over chemical methods for the industrial synthesis of dithionite, which include higher yields and purity, reduced cost, and fewer environmental and safety concerns.[1−4] This paper examines the nature of the cathodic limiting currents in buffered bisulfite solutions over a pH range of relevance to practical applications using rotating disk electrode (RDE) techniques. The results of these studies made it possible to determine the kinetics of the SO_2−HSO_3^- interconversion and to elucidate certain mechanistic aspects of this process.

Brief Background

The pH-dependent limiting currents on a dropping mercury electrode in acidified sodium sulfite solutions were described as early as 1930 by Gosman,[5] who attributed the most positive cathodic wave to the formation of dithionous acid with the current being limited by the slow protonation of bisulfite to yield H_2SO_3, regarded as the most likely electroactive species. Kolthoff and Miller[6] found similar waves in mildly acidic buffered solutions, but explained the limiting current behavior in terms of the slow tautomerization of sulfurous acid (H_2SO_3) prior to the electron transfer step. The importance of preceding protonation was later emphasized by Cermak,[7] although both the nature and the kinetics of the reaction were not clearly identified.

More recently, Reynolds and Yuan[8] reexamined this problem and concluded that the electroactive species in the range $1.3 < pH < 3$ is sulfur dioxide (SO_2). Several arguments appear to support their view. In particular, the existence of H_2SO_3 in any of its tautomeric forms has never been established even in a cryogenic matrix;[9] hence, if any of such species exist, their lifetime would be too short to account for the observed currents (see eqs 6 and 7 below). Also to be considered is the possibility of one of the two tautomers of bisulfite as the electroactive species; however, these species are found to be present in comparable concentrations in the pH range 2−6 and their equilibrium quotient does not show a significant pH dependence.[10,11] This behavior is not compatible with the experimentally observed decrease in the rate of the preceding chemical reaction with increasing pH, and with the eventual disappearance of the wave at pH 6, a value at which the concentration of bisulfite (pK_2 ca. 6.96) is still high.

Sulfur dioxide is known to undergo reversible reduction in strongly acidic media on a variety of electrode materials at around −0.4 V vs SCE;[6−8,12,13] it seems, thus, conceivable that at $pH > 3$, SO_2 is also the electroactive species in this potential region, as was recently proposed in this laboratory.[14] In this pH range, however, the amount of free SO_2 in the solution is low and the current would become limited by the rate of its formation from bisulfite (eq 1, Scheme 1). Sulfur dioxide

SCHEME 1

$$HSO_3^- + H^+ \leftrightarrow SO_2 + H_2O \quad (1)$$

$$SO_2 + e^- \leftrightarrow SO_2^{\bullet -} \quad (2)$$

$$2SO_2^{\bullet -} \rightarrow S_2O_4^{2-} \quad (3a)$$

$$\text{or} \quad SO_2^{\bullet -} + SO_2 \leftrightarrow S_2O_4^{\bullet -} \xrightarrow{e^-} S_2O_4^{2-} \quad (3b)$$

10.1021/jp983752c CCC: $18.00
Published on Web 03/03/1999

undergoes rapid one-electron reduction, to yield a radical, eq 2, which generates dithionite as the final product, either via fast dimerization, eq 3a, or SO_2 addition followed by a subsequent electron transfer, eq 3b. The latter two processes are analogous to those found in aprotic solvents[15] and will not be pursued in this work; rather, the purpose of the present investigation is to get further insight into the mechanism and kinetics of SO_2 formation from bisulfite, i.e., eq 1 in Scheme 1.

Theory

The reaction mechanism of relevance to this work, known as chemical−electrochemical (CE), involves the reduction (or oxidation) *on the electrode*, of a species produced by a preceding chemical reaction in the bulk solution, and may be represented as follows:

SCHEME 2

$$X \underset{k_b}{\overset{k_f}{\rightleftharpoons}} Y \quad \text{in the solution} \tag{4}$$

$$Y \rightarrow Z \quad \text{on the electrode} \tag{5}$$

In this scheme, X is the solution-phase, electrochemically inactive species in the potential range of interest that generates the actual redox active species Y, and k_f and k_b are the forward and backward rate constants for the corresponding reactions in eq 4. This model would be applicable to Scheme 1, eqs 1−3, for $X \equiv HSO_3^-$; $Y \equiv SO_2$, and $Z \equiv S_2O_4^{2-}$, provided the media are well buffered, so that the reaction in eq 1 may be regarded as pseudo first order.

Reactions that proceed via a CE mechanism, for which the rates of the forward and/or backward reactions in eq 4 are fast compared to the rate of diffusion (see details in refs 16 and 17 and also in the Appendix), will elicit limiting currents at a RDE controlled by the kinetics of the homogeneous process, as opposed to pure convective diffusion. An analytical solution to this problem, within Levich's mass transport model, was first reported by Koutecky and Levich,[16] and shortly thereafter, generalized by Dogonadze[17] to include the case of unequal diffusion coefficients for X and Y. A further extension of this formalism to account for currents below limiting values is given in the Appendix. Compton and Harland[18] calculated limiting currents of CE processes using numerical techniques and found good agreement with the previously reported analytical solutions for fast reactions.

Based on Dogonadze's derivation[17] (see also eq A19 in the Appendix), the dependence of the limiting current, i_{lim}, on the rotation rate ω of the RDE for a CE mechanism can be written as follows:

$$1/i_{lim} = 1/u + 1/(a\omega^{1/2}) \tag{6}$$

Since $K = [SO_2]/[HSO_3^-] = [Y]/[X] = k_f/k_b \ll 1$ in the pH range examined in this work, the parameters u and a reduce to

$$u = nFC^0k_f(D_Y/k_b)^{1/2} \tag{6a}$$

$$a = (nFD_XC^0)/(1.61D_X^{1/3}\nu^{1/6}) \tag{6b}$$

where C^0 represents the sum of the bulk concentrations of X and Y. Note that a may be regarded as the Levich slope for a redox process involving the same number of electrons as for Y ($n = 1$ for eq 2), but for a species with the diffusion coefficient of X. Hence, plots of $1/i_{lim}$ vs $1/\omega^{1/2}$ are linear with intercepts $1/u$, the parameter that carries kinetic information. According to its definition, eq 6, u is independent of D_X and ν, but depends on C^0. An alternate means of analyzing these data involves a rearrangement of eq 6 suggested by Vielstich,[19] i.e.

$$i_{lim}/\omega^{1/2} = a - bi_{lim} \tag{7}$$

where a is the same as in eq 6 and $b = a/u = D_X^{2/3}D_Y^{-1/2}(Kk_b)^{-1/2}/1.61\nu^{1/6}$. In this case, a plot of $i_{lim}/\omega^{1/2}$ vs i_{lim} would give a straight line with a slope b, independent of C^0. Although this latter approach allows a clearer and more compact presentation of results, the Koutecky−Levich coordinates (eq 6) would be preferable for situations in which the solution viscosity varies within the set of measurements.

Experimental Section

Both the optical and electrochemical instrumentation have been described in detail in ref 14. A Ag/AgCl in 3 M NaCl (BAS) separated by a closed (wet) glass stopcock and connected to the working electrode compartment through a Luggin capillary was used as the reference electrode. A large area (4 cm^2) gold foil separated by a glass frit served as the auxiliary electrode. A bismuth electrode was selected for these studies to take advantage of its wide potential window and the relative ease by which clean surfaces can be prepared.[20] The bismuth RDE (0.295 cm^2) was fabricated by casting a Bi rod (99.999%, Alfa Aesar) into an epoxy matrix which was later machined to shape. Immersion of the Bi electrode into solution was done under potentiostatic control as described in ref 21. The citrate and acetate buffers were prepared using citric acid (ACS reagent, Aldrich), and trisodium citrate dihydrate (certified, Fisher) or sodium hydroxide (semiconductor grade, Aldrich), and glacial acetic acid (certified ACS+, Fisher), and sodium hydroxide or sodium carbonate (ACS certified), respectively. Sodium perchlorate hydrate (99.99%, Aldrich) was used as the background electrolyte. Water was obtained from an EASYpure UV purification system (Barnstead). In order to reduce the loss of volatile components from the solutions examined (SO_2 and acetic acid), the Ar gas used for deaeration was saturated with the vapor of the same solution in a bubbler. Measurements of pH were made using a glass electrode (Fisher) with a high-impedance pH meter (Chemcadet). Calibration was achieved using commercial standards with pH = 4.00 and 7.00. The cell used in this work was not thermostated; however, the room in which experiments were performed was equipped with microclimate control affording temperatures of 23.3 ± 0.3 °C.

In the course of our work it was found that the reduction of bisulfite on Bi, and other electrode materials as well, was sensitive to the presence of trace impurities, most likely organic surfactants in the solution, yielding in many instances tilted limiting currents of the type shown in ref 1. Larger and potential independent i_{lim} values could be restored momentarily, however, by repolishing the electrode with 0.05 μm alumina.

More detailed studies were performed in 10 mM solutions of sodium sulfite in citrate buffer (see below) at pH 4.20 to examine the effects of electrode potential and convection on the kinetics of inhibition of bisulfite reduction. To monitor changes in the polarization curves as a function of the total holding time, t_h, the electrode potential was held at a selected value E_h, either with or without rotation to allow impurities to adsorb, and scanned every 5 min at 20 mV/s, down to −1.1 V and then up to E_h, *while rotating at 3600 rpm*. No noticeable hysteresis nor tilted limiting currents could be found in the polarization curves between the scans in the positive and negative directions, indicating that, within the time scale and

potential range of the scan, the coverage of the surfactant remains essentially constant. The values of the current at −0.9 V vs t_h were fitted to single-exponential decay functions. For example, for $E_h = -0.6$ V vs Ag/AgCl, i.e., the reported point of zero charge (pzc) of polycrystalline Bi,[20] the decay time constant, τ, for $\omega = 0$ and 3600 rpm, was 35 and 13 min, respectively. At more negative E_h values, τ increased, e.g. at −0.8 V and 0 rpm, $\tau = 73$ min. The enhanced inhibition observed under rotation and at potentials close to the pzc corroborates our suggestion that solution phase surfactants are responsible for this effect. Unfortunately, neither the concentration of the surfactant nor its coverage at a specific time is known. It is, nevertheless, instructive to estimate the first of these quantities assuming that adsorption occurs under diffusion-limited conditions with a sticking coefficient of unity and that a significant fraction of the surface is covered by the surfactant (1 nmol/cm^2) at $t = \tau$, e.g., 13 min at $\omega = 3600$ rpm. Based on this model and a diffusion coefficient for the surfactant of ca. 10^{-6} cm^2/s, its concentration in solution would be on the order of tens of pM. Very similar inhibitory effects were observed using a Bi rod in the hanging meniscus configuration RDE, i.e., without the epoxy shroud, suggesting that the soluble fractions of the resin are not the major source of contamination. We also found similar inhibition phenomena in other buffers (acetate, phosphate) and that the kinetics of the poisoning became slower at lower pH.

Complications derived from these contaminants could be avoided by polarizing electrodes at potentials at least 0.5 V negative to the pzc of Bi just prior to data collection to allow impurities to desorb. As judged by the results obtained in independent runs, the reproducibility of i_{lim} employing this pretreatment was better than ±3%.

Limiting currents as a function of ω, required for the kinetic analysis (see eqs 6 and 7), were recorded at fixed potentials by stepping ω in fixed increments (50−200 rmp), i.e., staircase scan method, in the range 200−8000 rpm toward both faster and slower rates, using computer-generated voltages as inputs to the Pine MSRX speed control and rotator. Five to 10 rotations, or 0.1 s, whichever was longer, were allowed for the disk currents to achieve steady state before data were acquired. This ω vs time program allows the most expedient means of collecting steady-state data over a given ω range (for a fixed ω increment), as shown by Miller and co-workers[22] for a similar technique, in which ω was ramped exponentially using an analogue signal generator.

Results

Figure 1 shows polarization curves obtained with a Bi RDE in 10 mM Na_2SO_3 in citrate buffer solutions of different pH in the range 3.09−5.36 at a scan rate of 10 mV/s and $\omega = 900$ rpm. As indicated, the values of i_{lim} for the electroreduction dropped significantly as the pH increased. The faradaic efficiency for dithionite production, as determined by in situ UV−visible reflection−absorption spectroscopy at a RDE,[14] was 100% down to the onset of hydrogen evolution, indicating that no further reduction or decomposition of this product occurs under these conditions.

Plots of $i_{lim}\omega^{1/2}$ vs i_{lim} obtained in the same solutions specified in the caption Figure 1 (see Figure 2) yielded straight lines with an intercept of -0.193 ± 0.005 mA cm^{-2} rpm$^{-1/2}$, which is equal to one-half of the Levich slope for the oxidation of bisulfite on gold measured in the *same* solution. The slopes of these lines, b (see eq 7), increased with pH, supporting the view that the rates of the preceding reaction, k_f, decrease as the solution becomes less acidic. In agreement with theoretical predictions (see eq 7), the intercepts, a, at fixed pH, were found to vary linearly with the concentration of bisulfite in the range 2−50 mM (not shown in this work), whereas the slopes remain unaffected.

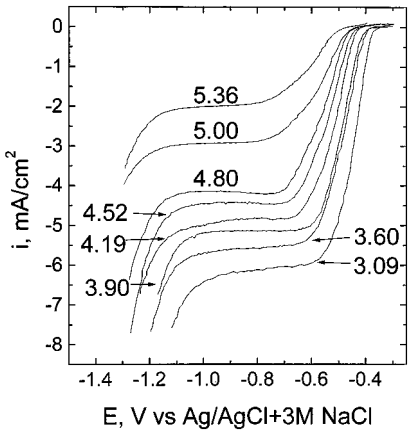

Figure 1. Polarization curves for bisulfite reduction obtained with a Bi RDE in 0.10 M citric acid + xM NaOH + (0.50 − x)M $NaClO_4$ + 10 mM Na_2SO_3 solutions, at the specified pH values ($0.1 < x < 0.4$). Rotation rate $\omega = 900$ rpm. Scan rate: 10 mV/s.

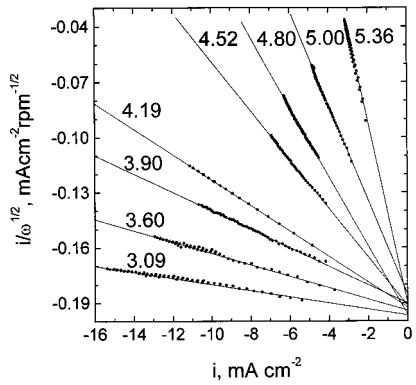

Figure 2. Representative $i_{lim}\omega^{1/2}$ vs i_{lim} plots obtained from data recorded in the same solutions specified in caption Figure 1 at the pH values indicated.

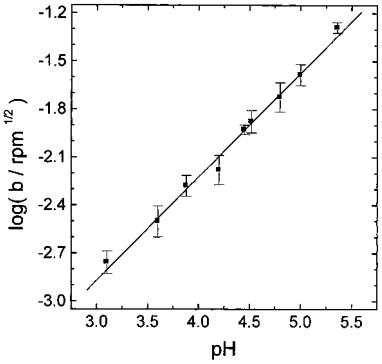

Figure 3. Logarithm of the kinetic parameter b obtained from the slopes of the lines in Figure 2 as a function of pH.

The pH dependence of the kinetic parameter b was found to be linear in log coordinates (see Figure 3); the slope of the line, however, was closer to $^2/_3$ rather than 1, as would be expected for the mechanism shown in eq 1, Scheme 1, suggested in the Introduction. Not considered in that reaction sequence was the possibility that undissociated acid may also serve as a proton donor, i.e., a general acid catalysis route. In such a case,

$$k_f = k_f^{H}[H_3O^+] + k_f^{HA}[HA] \qquad (8)$$

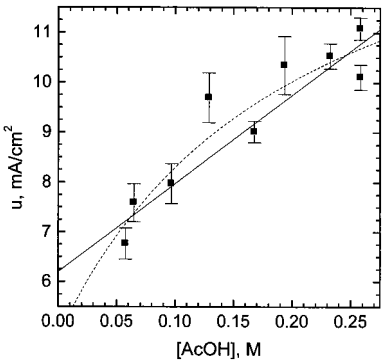

Figure 4. Rate constant of conversion of HSO_3^- into SO_2 (see eq 9) as a function of the concentration of free acetic acid [AcOH] in solutions of (0.288*x*)M AcOH + *x* M AcONa + + (0.5 − *x*) M $NaClO_4$ + 10mM Na_2SO_3 at constant pH 5.30. For $x > 0.5$ M no perchlorate was added. The error bars show standard deviations observed with 20 consecutive rotation rate scans in the same solution. Solid line: linear fit; dashed line: non linear fit. See text for discussion.

which combined with eq 6a would yield,

$$u = nFCD_Y^{1/2}\{(k_b^{1/2}/K_1)[H_3O^+] + (k_f^{HA}/k_b^{1/2})[HA]\} = p[H_3O^+] + q[HA] \quad (9)$$

where $K = k_b/k_f^H$ is the equilibrium constant $[H_3O^+][HSO^-]/[SO_2]$. This type of catalysis has been found, for example, for the protonation of pyruvate with imidazolinium cation yielding the electroactive pyruvic acid, as shown by Becker and Strehlow using polarography.[23]

Further insight into this issue was gained by performing experiments of the same type described above at fixed pH, 5.30, and fixed ionic strength, 0.50 M,[24] in acetate buffer solutions of varying buffer capacities. The results obtained showed a gradual decrease in the magnitude of *a* from −0.21 to −0.17 mA $rpm^{1/2}/cm^2$ as the concentration of acetate buffer increased from 0.06 to 1.21 M, owed most likely to a gain in solution viscosity, whereas *b* decreased more markedly, from 0.030 to 0.015 $rpm^{-1/2}$. The ratio $a/b = u$ as a function of concentration of free acetic acid [AcOH] is shown in Figure 4. Despite some scatter, the quality of the data obtained with the staircase rotation rate scan method appears superior to all previous studies of protonation reactions involving voltammetric methods,[25] indicating beyond a doubt that the rate of protonation increases with [AcOH]. A linear regression of the data, shown in Figure 4, yielded $p = (12.3 \pm 0.9) \times 10^5$ mA cm^{-2} M^{-1} and $q = 17.7 \pm 2.3$ mA cm^{-2} M^{-1}. From these values, and using literature data for $K_1 = 10^{-1.86}$ M[26] and $D_Y = 1.8\ 10^{-5}$ cm^2/s,[27] obtained at the same ionic strength, the values of all the relevant rate constants can be estimated, namely, $k_b = (1.6 \pm 0.2) \times 10^7$ s^{-1}, $k_f^H = (1.2 \pm 0.15) \times 10^9$ M^{-1} s^{-1} and $k_f^{HA} = (1.7 \pm 0.5) \times 10^4$ M^{-1} s^{-1}.

Two-dimensional linear regression of *u* as a function of both $[H_3O^+]$ and [AcOH] in the pH range 4.5−5.5 and [AcOH] 0.05−0.6 M, comprising a total of 20 points, including those in Figure 4, yielded $p = (12 \pm 7) \times 10^5$ mA cm^{-2} M^{-1}, $q = 25 \pm 6$ mA cm^{-2} M^{-1}, and an intercept of -0.6 ± 4 mA cm^{-2}. Larger standard deviations in this case are caused by a weaker dependence of *u* on [AcOH] relative to $[H_3O^+]$ at lower pH, as well as a possible dependence of these values on $[A^-]$ to be considered further in the Discussion section. The small value of the intercept suggests that water does not contribute significantly to the total rate of bisulfite protonation.

Discussion

The values of the rate constants obtained in this work were found to be comparable to those reported by other groups using different experimental techniques, as summarized in Table 1.

Not listed in this table is the value of $k_f^H = 3.7 \times 10^8$ $M^{-1}s^{-1}$ obtained from polarographic measurements[8] closely related to our technique.

Also of interest is to compare various aspects of the SO_2/HSO_3^- reaction with a chemically similar, albeit much slower transformation, namely the hydration of carbon dioxide to bicarbonate ion, CO_2/HCO_3^-, for which the intermediate, H_2CO_3, can be easily identified.[30] If the SO_2/HSO_3^- reaction is assumed to proceed via Scheme 3

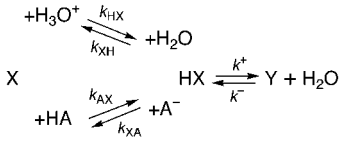

(10)

(see below, where $SO_2 \equiv Y$ and $HSO_3^- \equiv X$), a mechanism that involves the same corresponding intermediate, i.e., H_2SO_3 (HX), the data presented in this work enables some of its kinetic and thermodynamic properties to be estimated. Although this scheme ignores the existence of tautomeric forms of both bisulfite and sulfurous acid, it can be used as a working model as illustrated by Eigen and co-wokers.[28]

For carbonic acid, the rate of dissociation k_{XH} is higher than the rate of dehydration k^+;[30] hence, one can expect a similar behavior for sulfurous acid, since in both cases dissociation involves fewer structural changes than dehydration. The consistency of this assumption will be verified below. This approach allows one to consider the formation of HX as a preequilibrium step yielding the following relationships:

$$k_b = k^- \quad (11)$$

$$k_f = k^+ \frac{\frac{k_{HX}}{k_{XH}}[H_3O^+] + \frac{k_{AX}}{k_{XH}}[HA]}{1 + \frac{k_{XA}}{k_{XH}}[A^-]} \quad (12)$$

It is evident from these equations that the linear dependence of *u* on [AcOH] proposed in the Results section, eq 8, is equivalent, in this microscopic model (Scheme 3), to the condition $k_{XA}[A^-]/k_{XH} \ll 1$; then, from eqs 8 and 12

$$k_f^H = k^+ k_{HX}/k_{XH} \quad (13)$$

$$k_f^{HA} = k^+ k_{AX}/k_{XH} \quad (14)$$

It will be assumed in what follows that this is the case, since it agrees with the experimental data, and the issue of consistency will be discussed later in this section.

Based on our experimental results and eqs 13 and 14

$$k_{HX}/k_{AX} = k_f^H/k_f^{HA} \approx 7 \times 10^4 \quad (15)$$

A further analysis of these results is possible only if additional assumptions concerning the rate constants are introduced. In particular, some of the reactions in Scheme 3 are likely to be diffusion controlled, and, therefore, their rate constants, as discussed by Crooks,[31] can be estimated. For example, the rates of protonation of oxoanions by hydronium cation have rate

TABLE 1: Comparison of k_b and k_f^H Obtained in This Work with Those Reported in the Literature

reaction	rate const	Eigen et al.[28] [a]	Betts and Voss[29] [b]	this work
$SO_2 + H_2O \rightarrow HSO_3^- + H^+$	k_b (s^{-1})	3.4×10^6	1.1×10^8	1.6×10^7
$HSO_3^- + H^+ \rightarrow SO_2 + H_2O$	k_f^H (M^{-1} s^{-1})	2×10^8	2.5×10^9	1.2×10^9

[a] From ultrasound absorption in acidic solutions. [b] From oxygen isotope exchange rates in alkaline solutions.

constants of ca. 2×10^{10} M^{-1} s^{-1},[24] which can then be regarded as a good approximation for k_{HX}, and, therefore, yield from eq 15 $k_{AX} \approx 3 \times 10^5$ M^{-1} s^{-1}.

The magnitude of k_{AX} is far below the diffusion-controlled limit, indicating that sulfurous acid is stronger than acetic acid and, as also discussed by Crooks, that the reverse reaction, i.e., proton abstraction by acetate anion from neutral sulfurous acid, should be diffusion controlled. Typical rate constants for protonation of oxoanions by stronger acids are about 1×10^{10} M^{-1} s^{-1}.[31] Assigning this latter value to k_{XA}, the ratio of dissociation constants of the two acids can now be calculated:

$$k_{XA}/k_{AX} = K_{HX}/K_{HA} = [HSO_3^-][AcOH]/[H_2SO_3][AcO^-] = 3 \times 10^4$$

Using $K_{HA} = 10^{-4.75}$ M,[32] one obtains $K_{HX} = 0.6$ M and, hence, $k_{XH} = K_{HX}k_{HX} = 1 \times 10^{10}$ s^{-1}.

Sillen's compilation[32] lists two values for K_{HX}: 0.35 M, attributed to Kolthoff,[33] and 0.040 M, claimed by Flis et al.;[34] however, both these entries appear unreliable. In particular, Kolthoff used the notation H_2SO_3 to refer to what is currently regarded as the sum of free dissolved SO_2 and the acid, and, therefore, did not introduce pK_{HX}. Rather, he used the pK reported in an earlier publication (1.74×10^{-2} M), which matches that currently accepted for $K_1 = [H^+][HSO_3^-]/[SO_2]$.[26] On this basis, the entry in Sillen's monograph is difficult to justify. In fact, the actual value listed in those tables does not appear explicitly in Kolthoff's publication. Later, Flis et al.[34] examined solutions obtained by dissolving SO_2 in water using iodometry to determine the total concentration of S(IV). In such unbuffered media, the net reaction would yield equal concentrations of hydronium ions and bisulfite; hence, the equilibrium concentration of bisulfite can be determined from pH measurements using appropriate corrections for activity coefficients. The difference between the total S(IV) concentration and bisulfite would then equal the sum of SO_2 and H_2SO_3. By assuming that the UV absorption band centered at 277 nm is due solely to SO_2 (and not to HSO_3^- or H_2SO_3), its concentration could be measured by spectrophotometric techniques and, thus, by subtraction, that of H_2SO_3. According to these authors a significant amount of H_2SO_3 should be present in equilibrium with SO_2 at pH lower than 2. This observation, however, was not confirmed by Raman spectroscopy.[11,35] A likely source of error in that publication lies in the calculation of $[HSO_3^-]$ from pH measurements. A more rigorous approach to estimate activity coefficients was used by Huss and Eckert[36] to study equilibria in aqueous SO_2 solutions by very similar iodometric, UV absorbance, and conductance measurement techniques who found no evidence for the presence of H_2SO_3.

On the basis of empirical thermodynamic correlations analysis and simple molecular calculations, Guthrie[37] obtained $k_{HX} = 0.005$ M for $SO(OH)_2$ and 400 M for $HSO_2(OH)$. These data indeed show, in agreement with our conclusions, that sulfurous acid is stronger than acetic acid.

The last undetermined constant, k^+, can be determined from eq 13 yielding a value of 7×10^8 s^{-1}. The equilibrium constant $[H_2SO_3]/[SO_2] = k^-/k^+ = 2 \times 10^{-2}$ is close to 5×10^{-2}, attributed by Sillen to ref 31, but lower than 0.33 claimed in ref 34. Also $k_{XH} = 1 \times 10^{10}$ $s^{-1} \gg 7 \times 10^8$ $s^{-1} = k^+$, justifying, therefore, the assumption of preequilibrium formation of H_2SO_3.

The other assumption used in the foregoing kinetic analysis, i.e., negligible rate of deprotonation of sulfurous acid by acetate compared to the rate of dissociation, may not seem consistent with the results of the analysis (Scheme 3), since under the conditions shown in Figure 4, $k_{XA}[A^-]/k_{XH} \leq 0.7$ and, thus, not much smaller than 1. However, a nonlinear fit to the data shown in Figure 4 (dashed line) based on eq 6a, 11, and 12 yielded values for the microscopic rate constants, which, within their uncertainty, are not different than those obtained from the linear fit. Although the statistical analysis does not favor one model over the other, the experimental results clearly support a general acid catalysis mechanism.

Conclusions

Analysis of the limiting currents observed using a bismuth rotating disk electrode for the reduction of bisulfite to dithionite in mildly acidic buffered solutions is consistent with the reaction proceeding by a chemical electrochemical (CE)-type mechanism with sulfur dioxide being the reactive species. The kinetics of the preceding reaction, $HSO_3^- + H^+ \rightleftarrows SO_2 + H_2O$, was found to be dependent on pH and concentration of the buffer as prescribed by a general acid catalysis mechanism, i.e., both hydronium and undissociated acid serve as proton donors. On the basis of the values of the rates constants obtained in this work, H_2SO_3 may be characterized as a strong acid ($K_{HX} = 0.6$ M) which undergoes dehydration within a few nanoseconds, and, thus, explain its highly elusive character.

Acknowledgment. This work was supported in part by the Advanced Research Projects Agency, ONR Contract No. N00015-92-J-1848. The authors wish to express their appreciation to Prof. John Stuehr for interesting discussions.

Appendix

Current on the RDE in the Case of CE Process. The equations of mass balance at a RDE for an electrochemical process involving a preceding (pseudo)first-order homogeneous reactions 4 and 5 may be written as follows:

$$D_Y\frac{d^2Y}{dz^2} - v(z)\frac{dY}{dz} + k_f X - k_b Y = 0 \quad \text{(A1)}$$

$$D_X\frac{d^2X}{dz^2} - v(z)\frac{dX}{dz} + k_f X - k_b Y = 0 \quad \text{(A2)}$$

The appropriate boundary conditions in the bulk represent chemical equilibrium between X and Y

$$z \rightarrow \infty \qquad X + Y = C^0 \quad \text{(A3)}$$

$$z \rightarrow \infty \qquad k_f X - k_b Y = 0 \quad \text{(A4)}$$

The boundary conditions on the electrode will be referred to the case of constant surface concentration of Y and nonelec-

troactive X:

$$z = 0 \qquad Y = Y_S \tag{A5}$$

$$z=0 \qquad dX/dz = 0 \tag{A6}$$

For high Schmidt number $Sc = \upsilon/D_Y > 1000$, the normal component of the fluid velocity in the vicinity of the electrode can be approximated by $\upsilon(z) = -0.51\upsilon^{-1/2}\omega^{3/2} z^2$.[37] On this basis, and introducing a dimensionless coordinate normal to the electrode surface $\xi = z/\delta_Y$, where $\delta_Y = 1.61 D_Y^{1/3}\upsilon^{1/6}\omega^{-1/2}$, eqs A1 and A2 can be rewritten as

$$\frac{d^2Y}{d\xi^2} + \rho\xi^2\frac{dY}{d\xi} + \frac{\delta_Y^2}{D_Y}(k_fX - k_bY) = 0 \tag{A1a}$$

$$\frac{d^2X}{d\xi^2} + \rho\xi^2\frac{d_Y}{d_X}\frac{dX}{d\xi} - \frac{\delta_Y^2}{D_X}(k_fX - k_bY) = 0 \tag{A2a}$$

where $\rho = 1.61^3 \times 0.51 = 2.13$.

Let us multiply (A1a) by k_b and (A2a) by k_f and subtract one from the other

$$\epsilon^2\frac{d^2}{d\xi^2}(k_bY - k_fX) + \epsilon^2\rho\xi^2\frac{d}{d\xi}\left(k_bY - k_f\frac{D_Y}{D_X}X\right) - (k_bY - k_fX) = 0 \tag{A7}$$

where $\epsilon = \mu/\delta_Y$, $\mu^{-1} = [(k_f/D_X) + (k_b/D_Y)]^{1/2}$. Stretching of the independent variable $\xi = \chi\epsilon$ gives the "distinguished limit" form[39] for eq A7:

$$\frac{d^2}{d\chi^2}(k_bY - k_fX) + \epsilon^3\rho\chi^2\frac{d}{d\chi}\left(k_bY - k_f\frac{D_Y}{D_X}X\right) - (k_bY - k_fX) = 0 \tag{A8}$$

The parameter μ, known as the "reaction layer thickness",[16,17] has dimension of length and, as indicated above, depends on the rate constants of the preceding chemical reaction. If $\mu \ll \delta_Y$, i.e., the preceding chemical reaction is fast, $\epsilon \ll 1$, and can, therefore, be treated as a perturbation parameter and the term in ϵ^3 in eq A8 can be dropped as the first-order approximation.

$$d^2A/d\chi^2 - A = 0 \tag{A9}$$

where $A = k_bY - k_fX$. Note that a solution for nonequal diffusion coefficients can be obtained only within this approximation.

The other equation can be obtained by multiplying eq A2a by D_X/D_Y and adding eq A1a.

$$\frac{d^2}{d\xi^2}B + \rho\frac{D_Y}{D}\xi^2\frac{d}{d\xi}B = \frac{\rho}{\kappa}\xi^2\frac{d}{d\xi}A \tag{A10}$$

where

$$B = Y + (D_X/D_Y)X$$

$$D = \frac{k_bD_X + k_fD_Y}{k_b + k_f}$$

$$\kappa = \frac{k_bD_X + k_fD_Y}{D_Y - D_X}$$

The boundary conditions eqs A3−A6 then become

$$A(\xi\rightarrow\infty) = 0 \tag{A11}$$

$$B(\xi\rightarrow\infty) = (D/D_Y)C^0 \tag{A12}$$

$$A(0) = Y_S(k_b + k_f(D_Y/D_X)) - B(0)k_f(D_Y/D_X) \tag{A13}$$

$$A'(0) = k_bB'(0) \tag{A14}$$

The solution of eq A9 satisfying these boundary conditions is $A(\chi) = A(0)e^{-\xi/\epsilon}$; hence, eq A14 can be written as

$$A(0) = -k_b\epsilon B'(0) \tag{A14a}$$

The solution of eq A10 satisfying boundary conditions at $\xi = 0$, eqs A13 and A14 is given by

$$B(\xi) = B'(0)I(\xi) - \frac{\rho}{\epsilon\kappa}A(0)\int_0^\xi \exp\left(-\frac{t}{\epsilon}\right) \times \exp\left(\frac{1}{3}\frac{D_Y}{D}\rho t^3\right)t^2[I(\xi) - I(t)]\,dt + B(0) \tag{A15}$$

where in the latter formula

$$I(\xi) = \int_0^\xi \exp\left(-\frac{\rho}{3}\frac{D_Y}{D}t^3\right)dt$$

In order to analyze the boundary condition at $\xi \rightarrow \infty$ (A12), the integral in eq A15 should be expanded for small ϵ:[38]

$$\int_0^\infty \exp\left(-\frac{t}{\epsilon}\right)f(t)dt = \epsilon f(0) + \epsilon^2 f'(0) + \epsilon^3 f''(0) + ...$$

Using this result, eq A15 can be expressed as

$$B(\infty) = B'(0)\,I(\infty) + B(0) - 2I(\infty)(\rho/\kappa)A(0)\epsilon^2 + ... \tag{A16}$$

where $I(\infty) = (D/D_Y)^{1/3}$. Within the framework of the first-order solution discussed here, the ϵ^2 term in eq A16 should be dropped.

Expressions for $A(0)$, $B(0)$, and $B'(0)$ in terms of known parameters can be obtained by solving the system comprised of eqs A13, A14a, and A16. In particular, for $A(0)$ one obtains

$$A(0) = -k_bC^0\frac{K\frac{D}{D_Y} - \left(\frac{D_X}{D_Y} + K\right)\frac{Y_S}{C^0}}{\frac{D_X}{D_Y} + \frac{K}{\epsilon}\left(\frac{D}{D_Y}\right)^{1/3}} \tag{A17}$$

where $K = k_f/k_b$ as defined in eq 6a.

The final expression for the current can now be obtained, namely

$$i = nFD_Y\frac{dY}{dz}(0) = \frac{nFD_Y}{k_b\delta_Y}\frac{dA}{d\xi}(0) = -\frac{nFD_Y}{k_b\delta_Y\epsilon}A(0) = nF\frac{DC^0}{\delta}\frac{1 - \frac{1+K}{K}\frac{Y_S}{C^0}}{1 + \frac{1}{K}\frac{D_X}{D_Y}\frac{\mu}{\delta} +} \tag{A18}$$

where $\delta = \delta_Y(D/D_Y)^{1/3}$. In the case of limiting current conditions

($Y_S = 0$), eq A18 reduces to the Dogonadze's expression:[17]

$$i = \frac{nF\dfrac{DC^0}{\delta}}{1 + \dfrac{1}{K}\dfrac{D_X}{D_Y}\dfrac{\mu}{\delta}} \qquad \text{(A19)}$$

It is worth checking the range of ϵ for which eq A19 is valid by comparison with the results of numerical simulations.[18] In the case of equal diffusion coefficients Compton and Harland used a parameter k_A which is equal in our notation to ϵ^{-2} *(1/1.61*^{2} *×* *0.51*$^{2/3}$*)K/(1 + K)*. Based on Figure 1 in ref 18, one may conclude that the agreement between numerical solution and eq A19 is good for log $k_A > -0.5$ that is $\epsilon < 0.4$. For the case of unequal diffusion coefficients illustrated in Figure 2 of ref 18 one finds good agreement for the variable defined in ref 18, if

$$\frac{k_1 \upsilon^{1/3}}{\omega} = \frac{D_Y^{1/3}}{1.61^2}\frac{K}{1 + K\dfrac{D_Y}{D_X}}\epsilon^{-2} > 10^{0.66}$$

or, equivalently, $\epsilon < 0.009$.

For the system examined in this work ϵ was found to be smaller than 0.01 and, therefore, within the range of validity of this model.

References and Notes

(1) Scott, L. L.; Ding, Y.; Stadler, S. M.; Kohl, P. A.; Winnick, J.; Bottomley, L. A. *J. Electrochem. Soc.* **1998**, *145*, 4057.
(2) Oloman, C. *J. Electrochem. Soc.* **1970**, *117*, 1604.
(3) Gizetdinova, N. A. *J. Appl. Chem. USSR* **1980**, *52*, 2594.
(4) Cawlfield, D. W. USA Patent, 4,740,287 (1988).
(5) Gosman, B. *Collect. Czech. Chem. Commun.* **1937**, *2*, 185.
(6) Kolthoff, I. M.; Miller, C. S. *J. Am. Chem. Soc.* **1941**, *63*, 2818.
(7) Cermak, V. *Collect. Czech. Chem. Commun.* **1958**, *23*, 1871.
(8) Reynolds, W. L.; Yuan, Y. *Polyhedron* **1986**, *5*, 1467.
(9) Fleyfel, F.; Richardson, H. H.; Devlin, J. P. *J. Phys. Chem.* **1990**, *94*, 7032.
(10) Horner, D. A.; Connick, R. E. *Inorg. Chem.* **1986**, *25*, 2414.
(11) Littlejohn, D.; Walton, S. A.; Chang, S. G. *Appl. Spectrosc.* **1992,** *46*, 849.
(12) Jacobsen, E.; Sawyer, D. T. *J. Electroanal. Chem.* **1967**, *15*, 181.
(13) Benayada, A.; Bessiere, J. *Electrochim. Acta* **1985**, *30*, 593.
(14) Tolmachev, Y. V.; Wang, Z.; Hu, Y.; Bae, I. T.; Scherson, D. A. *Anal. Chem.* **1998**, *70*, 1149.
(15) Kim, B. S.; Park, S. M. *J. Electrochem. Soc.* **1995**, *142*, 26.
(16) Koutecky, J.; Levich, V. G. *Zh. Fiz. Khim.* **1958**, *32*, 1965.
(17) Dogonadze, R. R. *Zh. Fiz. Khim.* **1958**, *32*, 2437.
(18) Compton, R. G.; Harland, R. G. *J. Chem. Soc., Faraday Trans. 1* **1989**, *85*, 761.
(19) Vielstich, W. *Z. Anal.Chem.* **1960,** *173*, 84.
(20) (a) Palm, U.; Tenno, T. *J. Electroanal. Chem.* **1973,** *42*, 457. (b) Salve, M.; Palm, U. *Trans. Tartu University* **1974,** *332*, 71 and references therein.
(21) Tolmachev, Y. V.; Fedorovich, N. V. *Russ. J. Electrochem.* **1994**, *30*, 1368.
(22) Miller, B.; Bellavance, M. I.; Bruckenstein, S. *Anal. Chem.* **1972**, *44*, 1983−1992.
(23) Becker, M.; Strehlow, H. *Z. Electrochem.* **1969,** *64*, 42.
(24) For these studies the following solutions were used: (0.288*x*) M AcOH + *x* M AcONa + (0.5 − *x*) M $NaClO_4$ + 10 mM Na_2SO_3 at constant pH 5.30. For $x > 0.5$ M, for which the ionic strength was higher than 0.5 M no perchlorate was added.
(25) Strehlow, H. In *Techniques of Organic Chemistry*; Wessberger, A., Ed.; J. Wiley & Sons: New York, 1963; Vol. VIII, Part II, pp 799−844.
(26) Yakovlev, V. A.; Makarenko, V. A.; Poltoratskii, G. M. *J. Appl. Chem. USSR* **1989**, *62*, 1273.
(27) Samec, Z.; Weber, J. *Electrochim. Acta* **1975**, *20*, 413.
(28) Eigen, M.; Kustin, K.; Maass, G. *Z. Phys. Chem. NF* **1961**, *30*, 130.
(29) Betts, R. H.; Voss, R. H. *Can. J. Chem.* **1970**, *48*, 2035.
(30) Falcke, H.; Eberle, S. H. *Wat. Res.* **1990**, *24*, 685.
(31) Crooks, J. In *Comprehensive Chemical Kinetics*; Bamford, C. H., Tipper, C. F. H., Eds.; Elsevier: Amsterdam, 1977; Vol. 8.
(32) Bjerrum, J.; Schwarzenbach, G.; Sillen, L. G. *Stability Constants, Part I*; Chemical Society: London, 1957.
(33) Kolthoff, I. M. *Chem. Weekbl.* **1919**, *16*, 1154.
(34) Flis, I. E.; Arkhipova, G. P.; Mischenko, K. P. *Zh. Prikl. Khim.* **1965**, *38*, 1494.
(35) Meyer, B.; Ospina, M.; Peter, L. B. *Anal. Chim. Acta* **1980**, *117*, 301.
(36) Huss, A.; Eckert, C. A. *J. Phys. Chem.* **1977**, *81*, 2268.
(37) Guthrie, J. P. *Can. J. Chem.* **1979**, *57*, 454−457.
(38) Levich, V. G. *Physicochemical Hydrodynamics;* Prentice Hall: Englewood Cliffs, NJ, 1962.
(39) Nayfeh, A. H. *Introduction to Perturbation Techniques;* Wiley: New York, 1981.